Lithium selective adsorption on low-dimensional TiO_2 nanoribbons

Qin-Hui Zhang, Shao-Peng Li, Shu-Ying Sun, Xian-Sheng Yin, Jian-Guo Yu
State Key Lab of Chemical Engineering, East China University of Science and Technology, Shanghai, P. R. China, qhzhang@ecust.edu.cn

ABSTRACT

Mesoporous titania nanoribbons were synthesized via an optimized soft hydrothermal process and the derived titania ion-sieves with lithium selective adsorption property were accordingly prepared via a simple solid-state reaction between Li_2CO_3 and TiO_2 nanomaterials followed by the acid treatment process to extract lithium from the Li_2TiO_3 ternary oxide precursors. First, mesoporous titania nanoribbons were prepared and the formation mechanism was discussed; Second, the physical chemistry structure and texture were characterized by powder X-ray diffraction (XRD), (high-resolution) transmission electron microscopy (TEM/HRTEM), selected-area electron diffraction (SAED) and N_2 adsorption-desorption analysis (BET); Third, the lithium selective adsorption properties were studied by the adsorption isotherm, adsorption kinetics measurement and demonstrated with the distribution coefficient of a series of alkaline and alkaline-earth metal ions.

Keywords: adsorption; ion-sieve; lithium; low-dimensional; nanoribbons; titania

1 INTRODUCTION

Low-dimensional TiO_2-related materials with high morphological specificity, such as nanotubes, nanowires, nanosheets, nanofibers and nanoribbons had attracted particular interests in advanced application as catalyst [1], semiconductors for solarenergy conversion [2], gas sensors [3] and electrochemical materials [4], as it was discovered by Kasuga [5]. However, doubts exist concerning the formation and construction of these low-dimensional TiO_2-related materials [6, 7], and the lithium selective adsorption into titania ion-sieves from aqueous resources including brine or sea water has been rarely studied.

In this paper, the optimized synthesis, characteristic and consequent lithium ion-sieve property of titania nanoribbon were systematically studied. First, the optimized synthesis, with a direct soft chemical hydrolysis from TiO_2 nanoparticles to large quantities of quite uniform titania nanoribbons, was realized and the titania ion-sieves were accordingly prepared via a solid-state reaction followed by the acid treatment process to extract lithium from the Li_2TiO_3 precursor. Second, the structure and texture characteristics were characterized by XRD, TEM/HRTEM, SAED and BET analysis; Third, the lithium selective adsorption properties were studied by the batchwise adsorption isotherm and demonstrated with a series of alkaline and alkaline-earth metal ions, including Li^+, Na^+, K^+, Ca^{2+} and Mg^{2+}.

2 EXPERIMENTAL

2.1 Synthesis of titania nanoribbons and lithium ion-sieves

All chemicals used in this work were AR reagents, except where otherwise indicated. P25 (5 g, from Degussa Co. Ltd.) and an aqueous solution of NaOH (10 mol·l^{-1}, 500 ml) were mixed for 0.5 h in an ultrasonic bath, then transferred into a Teflon-lined stainless steel autoclave, sealed, and maintained at 448 K for 48 h; after the reaction was completed, the resulted white precipitate was separated by filtration and washed with 0.1 mol·l^{-1} hydrochloric acid solution and deionized water until the conductance of the supernatant lucid solution reached the same level with the deionized water (the pH value now is 7), followed by ultrasonic assisted dispersion in anhydrous ethanol for 0.5 h and dried at 333 K for 8 h. By optimizing the NaOH concentration and the reaction conditions of hydrothermal process, titania nanoribbons could be produced by using different particle size (from several nanometers to several hundreds of micrometers) of the starting anatase or rutile TiO_2 powder.

The as-synthesized titania nanoribbons (denoted as TO) were mixed with Li_2CO_3 with a molar ratio of 1:1, and calcined at 1173 K for 24 h in static air to insert the lithium into the Ti-O lattice and finally to form the Li_2TiO_3 tenary oxide precursors (denoted as LTO); the lithium extraction from Li_2TiO_3 precursors was carried out in 0.1 mol·l^{-1} HCl solution at 333 K for 72 h until the lattice lithium was completely extracted (in situ Measured by Metrohm 861 IC with Mrtrosep C2 100/4.0 column); the acid-treated materials were filtered, washed with deionized water and dried at 333 K for 8 h to obtain the final titania ion-sieves (denoted as STO).

2.2 Characterization of samples

The bulky phase of the samples were examined by powder XRD analysis on a Rigaku D/max 2550 X-ray diffractometer with monochromatized CuKα radiation (λ = 1.54056 Å), operating at 40 kV, 100 mA and scanning rate of 10° · min-1; The pore structure of the derived aggregates was characterized by N_2 adsorption at 77 K using an adsorption apparatus (Micromeritics, ASAP 2010 V5.02); surface area of the samples was determined from the

NSTI-Nanotech 2008, www.nsti.org, ISBN 978-1-4200-8503-7 Vol. 1

Brunauer-Emmett-Teller (BET) equation and pore volume, from the total amount of nitrogen adsorbed at relative pressures of ca. 0.96; The microstructure and morphology of the samples were analyzed using a low-magnification JEOL JEM-1200EX TEM (60 kV) and the layered structure of the nanoribbons was revealed by HRTEM and SAED on a JEOL JEM-2100F TEM (200 kV) after the samples were dispersed by ultrasonic in anhydrous ethanol for 10 min and then placed onto the cuprum grid for observations.

2.3 Lithium selective adsorption measurement

The lithium ion adsorption isotherm was carried out by stirring (130 r·min^{-1}) 100.0 mg titania ion-sieves in 50.0 ml LiCl solution (pH = 9.19, adjusted by buffer solution comprised of 0.1 mol·l^{-1} NH_4Cl and 0.1 mol·l^{-1} $NH_3 \cdot H_2O$, the molar ratio equal to 2.0) with different initial Li^+ concentration for about 144 h at 303 K till the attainment of equilibrium and the Li^+ content in supernatant lucid solution was determined in situ by IC; the exchange capacity or the amount of Li^+ adsorbed per gram of TiO_2 ion-sieve was calculated according to equation (1):

$$Q = (C_0 - C_e) \cdot V / W \quad (1)$$

in which, Q is the amount of metal ion adsorbed per gram adsorbent, mmol·g^{-1}; C_0, the initial concentration of metal ions, mol·l^{-1}; C_e, equilibrium concentration of metal ions, mol·l^{-1}; V, solution volume, ml; W, adsorbent weight, g.

The uptake behaviors of lithium ions compared with other ions in brine or seawater was carried out by stirring 100.0 mg of the ion-sieves in 10.0 ml solution (pH = 9.19) containing Li^+, Na^+, K^+, Ca^{2+} and Mg^{2+} of about 10 mmol·l^{-1}, respectively, for 144 h at 303 K till the attainment of equilibrium and the metal ions in supernatant lucid solution were also determined in situ by IC; The distribution coefficient (K_d) and separation factor (α^{Li}_{Me}) were calculated according to equation (2) and (3):

$$K_d = (C_0 - C) \cdot V / (C \cdot W) \quad (2)$$

$$\alpha^{Li}_{Me} = K_d(Li) / K_d(Me) \quad \text{Me: Li, Na, K, Ca and Mg} \quad (3)$$

3 RESULTS AND DISCUSSION

The Powder XRD diffraction patterns of the nanoribbon TiO_2 oxide, Li_2TiO_3 ternary oxide precursor and TiO_2 ion-sieve are presented in Figure 1.

Figure 1 TO give the pattern of the as-synthesized titania nanoribbons. The relatively broad Bragg peaks, due to the finite size of the particles, could not be assigned to the anatase, rutile or any known phase of titania in JCPDS card, nevertheless, the strong reflection peak at low degree of 2θ = 11.06 ° might correspond to the interlayer (or tunnel-tunnel) spacing of titania with a long-range ordered structure; combined with TEM/HRTEM analysis shown in Figure 2 (TO) and 3, it was indexed as a kind of layered or tunnel-constructed titania units.

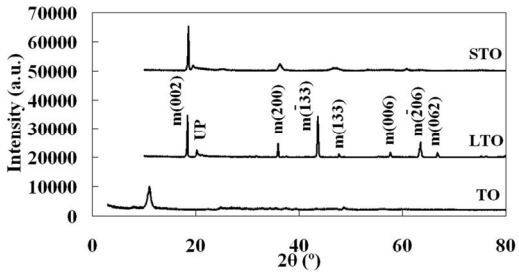

Figure 1: Powder XRD patterns of the nanoribbon TiO_2 oxide, Li_2TiO_3 precursor and derived TiO_2 ion-sieve. m (hkl): monoclinic Li_2TiO_3 crystal face; UP: unknown phase.

The XRD patterns of Figure 1 LTO were indexed to almost pure monoclinic phase [S.G.: C2/c (15)] of Li_2TiO_3 (JCPDS 33-831, a = 5.069Å, b = 8.799 Å, c = 9.759 Å), although there existed a faint unknown peak at 2θ = 20.24º. All the peaks became sharper than those of TO, indicating larger size distribution than the tiania nanoribbons as shown in Figure 2, which was resulted from the high temperature calcinations during the lithium insertion into Ti-O lattice procedure.

Figure 1 STO was of the derived titania ion-sieves. The reflection patterns of STO ion-sieve were somewhat similar to those Li_2TiO_3 precursor in Figure 1 LTO with broader and weaker peaks, however, they should not be indexed as monoclinic Li_2TiO_3 since nearly 96.5% of the lithium in Li_2TiO_3 had been extracted during the acid treatment process, quantitatively measured by in situ IC; and any known titania in JCPDS card was not matched. It implied that, although the Li^+ extracted from the titania nanoribbon derived Li_2TiO_3 precursor resulted in smaller lattice dimension (with the reflection peaks shifting a little to lower degrees), the Ti-O lattice in LTO precursor was very stable during the Li^+ extraction process and the locations of titanium in the crystal structure were well maintained. The specific characteristic arised partly from their rigid structure with little swelling or shrinking in aqueous phases and brought about a strong steric effect or an ion-sieve effect for various ions depending on the hydrated or dehydrated size of the adsorbed ions.

We carefully compared the synthesis process with those in the related literature, and confirmed the point of view of Li et al. [8] and Kasuga et al. [5, 6] that the washing and dispersing process was key to obtain the layered or tubular structure. In such earlier reports on one-dimensional titania nanostructures, the washing process merely with water would result mainly vesicles, shrinking under irradiation with an electron beam and finally changing to aggregate-like depositions. In this case, anhydrous ethanol was used to disperse the white precipitate after washing with HCl

solution and deionized water, and typical low-magnification TEM image was shown in Figure 2 TO. Samples dispersed in ethanol yielded mainly monodisperse nanoribbons with 20-100 nm in width and several micrometers in length, implying that ethanol was a good dispersant and aided the formation of low-dimensional nanostructure. Additionally, the use of ethanol enabled the formation of aggregation-free titania nanoribbons with quite uniform geometry, evidenced by the pore-size distribution obtained from the Barrett-Joyner-Halenda (BJH) deposition curve (inset of Figure 2 TO), indicating that the ethanol washed and dispersed nanoribbons maintained a pore size distribution centered around 43.7 nm, with no other peaks in the range from 1 to 100 nm. The pore-size distribution, unlike the TEM observations, was obtained statistically, thus the appearance of the single broad peak was attributed to capillary condensation in the slit-shaped mesopores with parallel walls and implied the separation of most nanoribbons from one another although some of the nanostructures looked thicker than others.

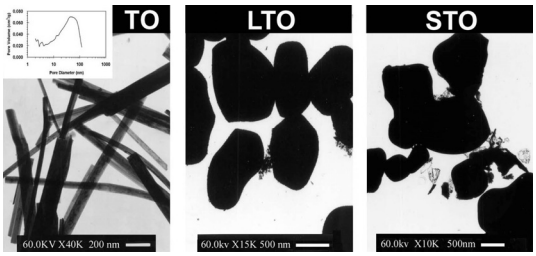

Figure 2: TEM images of TiO_2 oxides, Li_2TiO_3 ternary oxide precursors, and final TiO_2 ion-sieves.

HRTEM image (Figure 3-a) showed an individual nanoribbon with a rolled end; from the rolled region, it was clearly seen that the ribbon was very thin (<5 nm). Due to the limit of our current reaction apparatus, the effect of a temperature higher than 453 K would be further investigated; Figure 3-b was a typical HRTEM image of a nanoribbon with well-defined structure. Three sets of lattice fringes could be observed in the lattice resolved image with the face intervals of 0.79, 0.37 and 0.36 nm, respectively, exactly corresponding to the stripe images of the (200), (110) and (202) lattice plane (inset SAED pattern of Figure 3-b) of the monoclinic $H_2Ti_3O_7$. The fringes parallel to the (200) plane corresponded to an interplannar distance of about 0.79 nm and this fringe spacing was also comparable to the shell spacing (0.75-0.8 nm) of titania nanotubes reported recently [8, 9]. The other two sets of fringes, with smaller spacing of 0.36 and 0.37 nm, could be correspond to the (202) and (110) plane of the $H_2Ti_3O_7$ crystal structure; In many related reports to analyze the structure of the low dimension nanostructures, similar phenomena were discovered and described as $H_2Ti_3O_7{\cdot}xH_2O$ [9, 10, 11], $Na_xH_{2-x}Ti_3O_7$ [8], $H_2Ti_4O_9{\cdot}H_2O$ [12], and $H_2Ti_2O_4(OH)_2$ [13]. The SAED pattern also confirmed that the titania nanobibbons were single crystal.

After titania nanoribbons were calcinated with Li_2CO_3 to form Li_2TiO_3 at 1173 K for 24 h and treated with HCl solution for about 72 h to extract the lattice lithium, the obtained ion-sieve samples all changed to irregular particles with much larger size as shown in Figure 2 LTO and STO. This was resulted from the agglomeration during the high temperature solid reaction process and the lattice protons exchanged with lithium ions might also cause the destruction of hydrogen bonding, and as a result the low dimensional nanomaterials were destroyed to irregular particles, which was also evidenced in our related work focused on the effect of different polymorphs and the size effect of MnO_2 nanocrystals on the lithium ion extraction process from spinel $LiMn_2O_4$ [14].

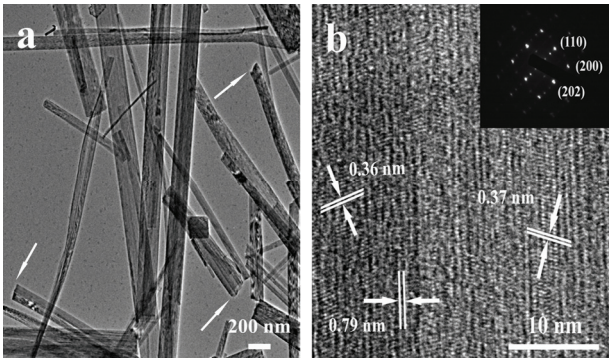

Figure 3: HRTEM images of one straight nanoribbon (a) and HRTEM (inset with SAED) image of a single titania nanoribbon growing along (200) (b).

The porosity of the ion-sieves should be closely related to their aggregation framework and Figure 4 showed the N2 adsorption-desorption isotherm of the derived ion-sieves. The nanoribbon derived ion-sieve STO had a much more alleviated desorption delay branch, an indication of the loosening of the aggregate structure, which might be resulted from the layered structure from the titania nanoribbons. Pore size distribution analysis via the DFT method, applicable for a complete range of pore size, was inserted in Figure 4, also indicating that the derived ion-sieves afforded a bimodal mesoporeous size distribution the peak pore size (D_p) centered around 3.9 and 11 nm of STO.

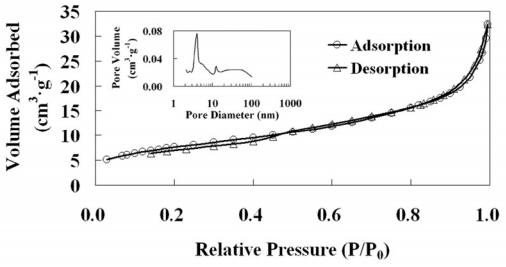

Figure 4: N_2 adsorption-desorption isotherms and pore distribution curves (insets) of the STO ion-sieves.

NSTI-Nanotech 2008, www.nsti.org, ISBN 978-1-4200-8503-7 Vol. 1

Figure 5 shows the Li^+ adsorption isotherm of STO ion-sieve and simulation according to Freundlich equation. The data present linearity with the congruence of $R^2 = 0.8765$, indicating that the Li^+ exchange process in the experiment is accorded with the Freundlich adsorption isotherm with the maximum Li^+ adsorption quantity to be 3.69 mmol·g^{-1}. The adsorption constants are calculated to be n = 12.56, K_f = 3.47 via the linear slope and intercept with the y-axis.

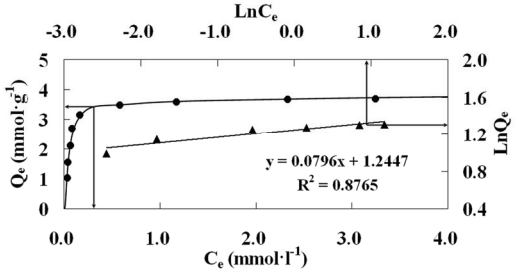

Figure 5: Li^+ adsorption isotherm of STO ion-sieve and simulation according to Freundlich equation. T = 303 K, pH = 9.19, V = 50 ml, W = 100 mg.

Metal Ion	Q_e mmol·g^{-1}	K_d ml·g^{-1}	α^{Li}_{Me}	CF 10^{-3}·l·g^{-1}
Li^+	0.997	13837.70	1.0	99.48
Na^+	0.044	20.83	664.3	17.25
K^+	0.003	0.31	45352.1	0.30
Mg^{2+}	0.209	17.00	814.0	14.53
Ca^{2+}	0.024	4.20	3294.0	4.03

Table 1: Li^+ adsorption selectivity on STO ion-sieves. T = 333 K, pH = 9.19, V = 10 ml, W = 0.10 g

Table 1 showed the selectivity of lithium ions compared with uptake behaviors for other typical alkaline and alkaline-earth metal ions in brine or sea water including Na^+, K^+, Ca^{2+} and Mg^{2+}. The equilibrium distribution coefficients (K_d) of lithium ion were 13837.7 of STO, and the selectivity of all metal cations was in the order of Li^+>> Na^+> Mg^{2+}> Ca^{2+}> K^+, indicating much higher selectivity for Li^+ than that of Na^+, K^+, Ca^{2+}, and Mg^{2+}; Additionally, the remarkable discrimination of the separation factor (α^{Li}_{Me}) between Li^+ and other cations (with the lowest multiple of 664.3) also meant that there existed no cross effect during the competitive adsorption process in the complex solution.

4 CONCLUSION

Titania nanoribbons with 20-100 nm in width and several micrometers in length were synthesized by a simple soft hydrothermal method (448 K for 48 h) followed by washing with HCl and deionized water and dispersing in ethanol. The equipment required was simple and alkali solutions were reusable, implying that this method had potential utilization for large-scale industrial production. Li_2TiO_3 precursor and final TiO_2 ion-sieves were prepared through the process of calcinations at 1173 K for 24 h, acid treatment with HCl for 72 h and dryness at 333 K for 8 h. According to XRD, TEM/HRTEM, SAED and BET characterization, the as-synthesized nanoribbons were mainly mesoporous monoclinic $H_2Ti_3O_7$ and the final TiO_2 ion-sieves were proved to have a remarkable lithium selective adsorption capacity, implying the promising application in lithium extraction from aqueous resources including brine or seawater with low lithium content, a novel utilization aspect for low-dimensional titania up to date.

5 ACKNOWLEDGEMENT

This work was supported by NSFC (No. 20576031 and 20576014), Risingstar Project (No. 05QMX1414) and National 863 Project (2008AA06Z111).

REFERENCES

[1] D. W. Bahnemann, S. N. Kholuiskaya, R. Dillert, A. I. Kulak and A. I. Kokorin, Appl. Catal., B: Environmental, 36, 161, 2002.
[2] A. Hagfeldt, M. Grätzel, Chem. Rev., 95, 49, 1995.
[3] Y. F. Zhu, J. J. Shi, Z. Y. Zhang, C. Zhang and X. R. Zhang, Anal. Chem., 74, 120, 2002.
[4] I. Moriguchi, R. Hidaka, H. Yamada, T. Kudo, H. Murakami and N. Nakashima, Adv. Mater., 18, 69, 2006.
[5] T. Kasuga, M. Hiramatsu, A. Hoson, T. Sekino and K. Niihara, Langmuir, 14, 3160, 1998.
[6] T. Kasuga, M. Hiramatsu, A. Hoson, T. Sekino and K. Niihara, Adv. Mater., 11, 1307, 1999.
[7] Y. C. Zhu, H. L. Li, Y. R. Koltypin, Y. R. Hacohen and A. Gedanken, Chem. Commun., 24, 2616, 2001.
[8] X. M. Sun and Y. D. Li, Chem. Eur. J., 9, 2229, 2003.
[9] G. H. Du, Q. Chen, R. C. Che, Z. Y. Yuan and L. M. Peng, Appl. Phys. Lett., 79, 3702, 2001.
[10] Q. Chen, W. Z. Zhou, G. H. Du and L.-M. Peng, Adv. Mater., 14, 1208, 2002.
[11] Y. Suzuki and S. Yoshikawa, J. Mater. Res., 19, 982, 2004.
[12] A. Nakahira, W. Kato, M. Tamai, T. Isshiki, K. Nishio and H. Aritani, J. Mater. Sci., 39, 4239, 2004.
[13] M. Zhang, Z. S. Jin, J. W. Zhang, X. Y. Guo, J. J. Yang, W. Li, X. D. Wang and Z. J. Zhang, J. Molec. Catal. A: Chem., 217, 203, 2004.
[14] Q. -H. Zhang, S. Y. Sun, S. P. Li and J. G. Yu, Chem. Eng. Sci., 62, 4869, 2007.